



Using chlorophyll fluorescence parameters and antioxidant enzyme activity to assess drought tolerance of spring wheat

S.V. OSIPOVA^{*,**,+} , A.V. RUDIKOVSKI^{*} , A.V. PERMYAKOV^{*} , E.G. RUDIKOVSKAYA^{*} , A.V. POMORTSEV^{*} , O.V. MUZALEVSKAYA^{**}, and T.A. PSHENICHNIKOVA^{***} 

*Siberian Institute of Plant Physiology and Biochemistry SB RAS, 664033 Irkutsk, Russia**

*Faculty of Biology and Soil, Irkutsk State University, 664003 Irkutsk, Russia***

*Institute of Cytology and Genetics SB RAS, 630090 Novosibirsk, Russia****

Abstract

The improvement of phenotyping methods is necessary for large-scale screening studies of wheat (*Triticum aestivum* L.) drought tolerance. The objective of our research was to find out whether it is possible to use chlorophyll (Chl) fluorescence parameters instead of biochemical indicators of drought tolerance when screening wheat. We measured shoot biomass, gas exchange, as well as biochemical and Chl fluorescence indicators in 11 wheat genotypes grown under contrasting water supplies and differing in drought tolerance. The effect of drought on the traits was evaluated using the effect of size index. We made two independent rankings: one based on biochemical indicators and the other on Chl fluorescence parameters. The positions of the three genotypes with the highest comprehensive drought tolerance index in the two independent rankings coincided completely. It is concluded that Chl fluorescence methods are suitable for identifying soft wheat genotypes that differ significantly in their ability to activate cellular defense mechanisms.

Keywords: ascorbate–glutathione cycle enzymes; chlorophyll fluorescence; comprehensive drought-tolerance index; proline; size of drought effect; sugars.

Highlights

- Eleven genotypes of spring soft wheat were ranked by their drought-tolerance indices
- The size of the drought effect on Chl fluorescence and biochemical traits was correlated
- Chl fluorescence is suitable for phenotyping physiological tolerance in wheat

Received 31 August 2023

Accepted 19 February 2024

Published online 1 March 2024

⁺Corresponding author

e-mail: svetlanaosipova2@mail.ru

Abbreviations: ABS – absorbance; APX – ascorbate peroxidase; Asc – ascorbic acid; Car – carotenoids content; Chl – chlorophyll; C_i – intercellular CO_2 concentration; DHAR – dehydroascorbate reductase; DM – dry mass; E – transpiration rate; ETR – rate of electron transfer; ETR_{max} – maximal electron transport rate; $F_{300\ \mu\text{s}}$ – fluorescence measured 300 μs after the start of illumination; F_t – terminal steady state of Chl a fluorescence; F_m – maximal Chl fluorescence; F_m' – maximal Chl fluorescence in leaves adapted to light; F_v/F_0 – ratio of photochemical to nonphotochemical quantum efficiencies; F_v/F_m – maximal photochemical efficiency of PSII; g_s – stomatal conductance; GR – glutathione reductase; I_k – the light intensity at which the alpha (α) and ETR lines intersect; PCA – principal component analysis; PI_{abs} – performance index at absorption basis; PI_{tot} – total performance index; P_N – photosynthetic rate; q_p – coefficient of photochemical fluorescence quenching; RC – reaction center; RC/ABS – efficiency indicator, expressed as the concentration of reaction centers in the total pool of chlorophyll; SB – main shoot biomass; SDE – size of drought effect; SOD – superoxide dismutase; V_i – relative value of variable fluorescence during phase I (30 ms); WUE – water-use efficiency ($= P_N/E$); α – the angle of inclination of the light curve characterizing the dependence of fluorescence on light intensity; Φ_{PSII} – effective quantum yield of PSII of photochemistry; ψ_0 – efficiency with which a trapped excitation can move an electron in the electron transport chain further than Q_A .

Acknowledgments: The research was carried out using the equipment of the Core Facilities Center ‘Bioanalitika’ at the Siberian Institute of Plant Physiology and Biochemistry SB RAS, Irkutsk, Russia. The work was supported by the budget Project of SIPPB SB RAS No. FWSS-2022-0002 and by the budget Project No. FWNR-2022-0017 of ICG SB RAS.

Conflict of interest: The authors declare that they have no conflict of interest.

Introduction

Drought tolerance is shaped by a large number of different adaptive mechanisms operating at different levels of plant organization (Nezhadahmadi *et al.* 2013, Oguz *et al.* 2022). Current programs focused on improving the agronomic drought tolerance of wheat involve selection among hundreds of promising genotypes (Sehgal *et al.* 2020). At the same time, it is believed that the best results can be obtained by an integrated strategy that takes into account both agronomic and physiological tolerance. The latter is understood as the ability of genotypes to withstand drought by mobilizing a variety of physiological mechanisms (Varshney *et al.* 2018).

Stability in the operation of the photosynthetic apparatus plays a key role in plant adaptation to adverse conditions. The antioxidant system response is one of the most studied physiological responses to drought, aimed at mitigating the damaging effects of reactive oxygen species on photosynthesis. The balance between the production of reactive oxygen species and their removal by antioxidant system components plays a crucial role in the processes of water conservation and biomass accumulation. Therefore, the knowledge available on this issue needs to be translated into stress management tools and methods (Rane *et al.* 2022). Among the antioxidant system components actively functioning in leaves, carotenoids (Car), superoxide dismutase (SOD), enzymes of the ascorbate–glutathione cycle are of great importance, as well as low-molecular-mass antioxidants – ascorbic acid and reduced glutathione. The pool of the latter two is supported by the activity of dehydroascorbate and glutathione reductases (DHAR and GR) (Ivanov *et al.* 2014, Rane *et al.* 2022). Soluble sugars whose protective functions are associated with the regulation of phytohormone biosynthesis can also act as direct antioxidants (Bolouri-Moghaddam *et al.* 2010, Sami *et al.* 2016). Given the role of proline in the redox balance and homeostasis of the cell, its content is often assessed in wheat screening studies (Szabados and Savouré 2010, Mwadzingeni *et al.* 2016, Peršić *et al.* 2022, Zhang *et al.* 2022).

To include physiological traits in large-scale omics or screening studies, it is necessary to develop and improve noninvasive high-throughput phenotyping methods. From this point of view, it is very attractive to adapt the Chl fluorescence parameters for such a purpose. They allow detection of changes in the operation of the photosynthetic apparatus under the influence of stress factors and are of great importance for predictive understanding of the reactions of photosynthetic apparatus to stress (Goltsev *et al.* 2016, Kalaji *et al.* 2017). Sieczko *et al.* (2022) used Chl fluorescence techniques to detect early changes in cucumber plants caused by phosphorus deficiency. Dąbrowski *et al.* (2023) showed that some Chl fluorescence parameters could serve as indicators for early detection of the effects of heavy metals such as cadmium and nickel.

Chl fluorescence methods have been used to assess drought tolerance of common winter wheat (Živčák *et al.* 2008, Peršić *et al.* 2022, Wang *et al.* 2022). In doing so,

different fluorescent indicators were recommended for inclusion in a comprehensive assessment of tolerance. Živčák *et al.* (2008) singled out the productivity index PI_{abs} as the most sensitive indicator of the stress state in winter wheat plants under water deficit. Peršić *et al.* (2022) concluded that the most reliable measure of the OJIP test for screening winter wheat seedlings was the PI_{tot} cumulative performance index. The same index was the most sensitive criterion when screening wheat plants in the field (Botyanszka *et al.* 2020). According to Botyanszka *et al.* (2020), parameters of fast Chl fluorescence can provide more accurate information on drought stress levels than data obtained by measuring spectral characteristics such as the normalized vegetation index NDVI. Begović *et al.* (2020), who studied the responses of winter barley plants to mild drought stress caused by adverse weather conditions, reached the same conclusion. Wang *et al.* (2022) proposed to include the NPQ parameter that reflects the level of nonphotochemical Chl fluorescence quenching and is an important photosynthetic apparatus protection mechanism, in the complex stability indexes. The Chl fluorescence methods continue to develop and are increasingly used as methods for high-throughput phenotyping of plant physiological tolerance to stress factors (Rapacz *et al.* 2019, Pleban *et al.* 2020, Pandey *et al.* 2021, Pshenichnikova *et al.* 2021, Peršić *et al.* 2022). At the same time, information is accumulated on the specificity of the response to stress conditions of primary photochemical reactions. Indicator of potential efficiency PSII (F_v/F_m), considered one of the reliable indicators of the photochemical activity of the photosynthetic apparatus, was not sensitive when wheat varieties and lines were grown under moderate light and water-scarcity conditions (Živčák *et al.* 2008, Osipova *et al.* 2019). The NPQ index associated with heat energy loss was informative in winter wheat only under severe drought stress in conditions of a significant decrease in the relative water content in leaves and an almost half-reduced photosynthetic rate (Živčák *et al.* 2013). We analyzed the sensitivity of Chl fluorescence parameters to water stress in wheat plants grown under moderate soil drought and more severe conditions combining atmospheric and soil drought. In this set of closely related genotypes, there were more than 70 recombinant lines created on the genetic basis of the Chinese spring variety. Popular Chl fluorescence indicators (F_v/F_m , Φ_{PSII} , and NPQ) were not informative regarding the level of drought stress, while rapid light-curve parameters changed in proportion to the level of stress load (Osipova *et al.* 2019). Thus, the sensitivity of Chl fluorescence parameters reflecting the photochemical activity of photosynthetic apparatus depends on the species, the stage of plant development, the type of stress, and the level of stress load.

We assume that changes in Chl fluorescence under water deficit conditions are associated with the defense responses of wheat plants at the cell level and probably with productivity. Consequently, Chl fluorescence methods offer a viable option for high-throughput phenotyping for drought tolerance in spring soft wheat.

Materials and methods

Plant material and experimental conditions: Four varieties of common spring wheat were used in the work: cv. Saratovskaya 29 (S29), which has constitutive drought tolerance; highly productive and moisture-loving cv. Yanezkis Probat (YP), as well as two old West Siberian spring wheat cultivars – Sibirka 1818 (Sib.) and Caezium 111 (Caez.). In addition, we used seven substitution lines created on the genetic basis of cv. S29. In the lines S29(YP 2A), S29(YP 2B), and S29(YP 2D), 2A, 2B, and 2D chromosomes of S29 were replaced by the corresponding chromosomes from YP. In the lines, S29(Sib. 2D) and S29(Caez. 2D), 2D chromosome of S29 was replaced by the homologues from Sib. and Caez. The lines S29(821 2A) and S29(483/98 2A) were created by replacing chromosome 2A of S29 with homologous chromosomes from *T. timopheevii* and *Aegilops markgrafii*. The effects of the substitution of these chromosomes on some biochemical indicators of drought tolerance have been described previously (Osipova *et al.* 2020).

The plants grew under controlled conditions of the *CLF PlantMaster* climate chamber (*CLF Plant Climatic GMBH*, Germany) installed in the phytotron of *SIFIBR SB RAS* with a 16-h photoperiod, a temperature of 23°C during the day and 16°C at night, an air humidity of 60%, and a light intensity of 300 $\mu\text{mol}(\text{photon})\text{ m}^{-2}\text{ s}^{-1}$. Ten grains of each genotype were sown in two Mitcherlich pots filled with soil (a mixture of humus, sand, and peat; 1:1:1). The soil water content in one pot was maintained at an optimal level (60% of the total soil moisture capacity). In the second pot, watering was limited to 30% of the total soil water capacity starting from the third leaf stage. The required soil moisture was maintained by weighing the pots. This drought pattern corresponds to spring droughts typical for the agricultural regions of Eastern and Western Siberia. Thus, the critical stages of spring wheat development – tillering and booting – proceeded under conditions of soil water deficiency. Photosynthetic parameters were measured at the stages of booting–beginning of heading. After the measurements, the main shoot was cut and weighed; the leave was saved for biochemical analysis. Flag leaves were frozen and stored at –80°C.

Some genotypes [S29, S29(YP 2A), S29(YP 2B), S29(YP 2D), S29(483 2A)] were grown in the greenhouse of the Institute of Cytology and Genetics, Siberian Branch of the Russian Academy of Sciences (Novosibirsk) under optimum and deficit rates of irrigation. Productivity components were studied in these genotypes.

Physiological and biochemical parameters: To determine the content of pigments, 50 mg of flag leaf tissue was homogenized in 3 ml of 80% acetone with 10 mg CaCO_3 . The homogenate was adjusted to 10 ml with 80% acetone, then centrifuged at $2,000 \times g$ for 10 min. A 3-ml aliquot of the supernatant was used to measure absorbance at 440.5, 648, and 664 nm using a *Hitachi U-1100* spectrophotometer (*Hitachi Ltd.*, Japan). The content of chlorophyll *a* (Chl *a*), *b* (Chl *b*), and Car was calculated using the formulas given

in the work of von Wettstein (1957). Pigment content was calculated as mg g^{-1} of dry leaf mass (DM).

Free proline content was measured spectrophotometrically (*Hitachi U-1100*, *Hitachi Ltd.*, Japan) at a wavelength of 520 nm using ninhydrin reagent according to the method of Bates *et al.* (1973). The content of water-soluble sugars in the leaves was determined by the anthrone method at a wavelength of 620 nm (Dische 1962). Proline content is presented as $\mu\text{mol g}^{-1}$ (DM), and water-soluble sugar content is given in mg g^{-1} (DM).

The maximal activity of dehydroascorbate reductase (DHAR, EC 1.8.5.1), ascorbate peroxidase (APX, EC 1.11.1.11), and glutathione reductase (GR, EC 1.6.4.2) was measured spectrophotometrically using an *Infinite M200 PRO* microplate reader (*Tecan Group Ltd.*, Switzerland) and *UV-Star* flat-bottom microplates (*Greiner Bio-One GmbH*, Germany). In all experiments, 10 μl of the enzyme extract was added to 200 μl of the total volume of the incubation medium. DHAR was analyzed in 50 mM potassium phosphate buffer, pH 7.0, containing 0.2 mM dehydroascorbate (*Sigma-Aldrich*, USA) and 2.5 mM GSH (*Reanal Private Ltd.*, Hungary). DHAR activity was judged by the increase in A_{265} in 1 min (extinction coefficient $E = 14 \text{ mM}^{-1} \text{ cm}^{-1}$) (Baier *et al.* 2000). A correction was made for the nonenzymatic reduction of dehydroascorbate. APX activity was determined by the decrease in A_{290} in a reaction medium containing 50 mM potassium phosphate buffer, pH 7.0, 0.5 mM of ascorbic acid (Asc) (*Sigma Aldrich*, USA), and 0.1 mM H_2O_2 ($E = 2.8 \text{ mM}^{-1} \text{ cm}^{-1}$) (Nakano and Asada 1981). A correction was made for the nonenzymatic oxidation of Asc by hydrogen peroxide. GR activity was determined by NADP(H) oxidation by monitoring the change in optical density at 340 nm for 1 min ($E = 6.2 \text{ mM}^{-1} \text{ cm}^{-1}$) in 50 mM potassium phosphate buffer, pH 7.8, containing 0.10 mM NADP(H) (*Sigma Aldrich*, USA) and 1 mM oxidized glutathione (*Reanal Private Ltd.*, Hungary) (de Lamotte *et al.* 2000). A correction was made for background absorbance at 340 nm in the reaction medium without NADP(H). The activity of DHAR, APX, and GR was expressed in micromoles of substrate per milligram of protein per min at 25°C. SOD activity (EC 1.15.1.1) was measured by inhibition of nitro blue tetrazolium (NBT) reduction by the method of Giannopolitis and Ries (1977). Each 200 μL of reaction medium contained 50 mM potassium phosphate buffer (pH 7.8), 13 mM methionine (*Reanal Private Ltd.*, Budapest, Hungary), 2 μM riboflavin (*Reanal Private Ltd.*, Hungary), 63 μM NBT (*Sigma Aldrich*, USA), 0.1 μM EDTA, and 10 μl of extract. A unit of SOD activity was defined as the amount needed to inhibit NBT reduction by 50%. Protein content was determined according to Bradford (1976) using BSA (*Sigma Aldrich*, USA) as a standard.

Gas exchange and Chl fluorescence emission parameters: The net photosynthetic rate (P_N), stomatal conductance (g_s), intercellular CO_2 concentration (C_i), and transpiration rate (E) were output from a portable leaf gas-exchange system *GFS-3000* (*Heinz Walz*, Effeltrich,

Germany). When measuring, the light intensity, CO₂ concentration, relative humidity, temperature, and airflow rate were set to PPF of 800 µmol m⁻² s⁻¹, 400 µmol mol⁻¹, 60%, 25°C, and 750 µmol s⁻¹, respectively. Water-use efficiency (WUE) was calculated as P_N/E .

The different aspects of Chl fluorescence measured were: (1) slow Chl fluorescence induction kinetics, (2) rapid light curves (RLC), and (3) fast Chl fluorescence induction kinetics (OJIP transient curve). Chl fluorescence was evaluated using a *PAM 2500* fluorometer (*Heinz Walz*, Effeltrich, Germany) integrated with *PamWin 3.05* software. A script was generated that allows to measure slow Chl fluorescence induction kinetics and rapid light curves on one sample. To record the minimal Chl fluorescence output in the dark-adapted state (F_0), we darkened the leaves for 30 min and then illuminated them with modulated measuring light of low frequency (5 Hz) and low intensity (630 nm). The Chl fluorescence intensity in closed reaction centers (F_m) conditions was measured after exposure to a high-intensity light pulse [25,000 µmol(photon) m⁻² s⁻¹, 630 nm wavelength, 0.1 s]. Red actinic light [677 µmol(photon) m⁻² s⁻¹] was used to maintain photosynthesis and achieve a steady state (F_i).

Based on the measured values of Chl fluorescence parameters, the *PamWin 3.50* program calculated Φ_{PSII} , q_P , ETR, and other parameters. We assessed the response to rapid increases in illumination (every 30 s) by exposing leaves to light intensities from 0 to 1,935 µmol m⁻² s⁻¹ PAR photons and took into account the initial slope of the fast light response curve (α), the maximal electron transfer rate (ETR_{max}), and the minimal saturation light intensity (I_k).

Chl fluorescence induced by a strong light pulse was digitized in the range of 0.1 to 300 ms in the 'View' device mode on the 'Fast kinetics' tab (Chen *et al.* 2013, Srivastava *et al.* 2021). Chl fluorescence induced by a strong light pulse was digitized in the range of 0.1 to 300 ms. The Chl fluorescence parameters discussed in the article are given in Appendix 1. All Chl fluorescence parameters measured and calculated in the study are described in Table 1S (*supplement*).

Statistics: An individual plant was taken as a biological replicate. SB was calculated as the average value for 10 plants. Gas exchange and Chl fluorescence parameters were measured in 6–8 plants of each genotype in two water regimes. Enzyme activity, pigments, soluble sugars, and free proline contents were measured for three plants per genotype in two water regimes, with each plant analyzed three times. Mean values for yield components were calculated from two independent replicates of seven plants each. The *Shapiro-Wilk* test was used to check the normality of the data distribution. The influence of soil drought on SB, biochemical, and Chl fluorescence parameters was assessed using the indicator 'size of effect' (Hedges, d) or, in our case 'size of drought effect' (SDE). It is based on differences between mean trait values under drought stress and control and takes into account sample size and pooled standard deviation (Hedges and Olkin 1985, Peršić *et al.* 2022). The d values were adjusted for small sample sizes.

The drought effect size (SDE) was calculated using the formulas:

$$d = (M_d - M_c) / SD_{pooled}$$

$$SD_{pooled} = \sqrt{[(N_d - 1) \times SD_d^2 + (N_c - 1) \times SD_c^2] / (N_d + N_c - 2)}$$

$$\text{Corrected (Hedges } d\text{)} = \text{SDE} = d \times [1 - 3 / (4 \times (N_d + N_c) - 9)]$$

M_d and M_c – mean values of traits in drought and control, respectively; SD_{pooled} – pooled standard deviation; SD_d and SD_c – standard deviation from mean values of traits under drought and control, respectively; N_d and N_c – sample size in drought and control, respectively.

The higher the size of the effect, the greater the increase in the parameter under drought conditions compared to the control. The negative values indicate a decrease in the parameter compared to the control. All calculations including means, pooled standard deviation, adjusted d value, and plotting were performed in *Excel* (Microsoft Corporation, 2010). Data distribution normality check and *Spearman* correlation analysis were performed using the *SigmaPlot 11* program (Systat Software, Inc, USA, 2008). The comprehensive drought tolerance index D of each genotype was calculated using principal components analysis (PCA) for the trait drought effect size values as follows (Deng *et al.* 2019):

$$D = \sum_{j=1}^n [U(X_j) \times W_j] \quad j = 1, 2, \dots, n$$

$$W_j = P_j / \sum_{j=1}^n P_j \quad j = 1, 2, \dots, n$$

$$U(X_j) = (X_j - X_{\min}) / (X_{\max} - X_{\min}) \quad j = 1, 2, \dots, n$$

$U(X_j)$ – the membership function values of each parameter; X_j – the j th composite index; X_{\min} – the minimal value of the j th composite index; X_{\max} – the maximal value of the j th comprehensive index; W_j – the importance of the j th comprehensive indicator in all of the composite indicators; P_j – the contribution rate of the j th comprehensive index of each genotype.

Principal component analysis (PCA) was performed using the *PAST* program (Hammer *et al.* 2001).

Results

The mean values of shoot biomass, biochemical indicators of tolerance, gas-exchange parameters, 33 Chl fluorescence parameters, and calculated drought effect size (SDE) for each trait are presented in Table 1S. SDE values varied significantly among genotypes. To identify the traits with the highest variability in SDE, principal component analysis (PCA) was applied.

PCA for SDE on physiological and biochemical traits: The following traits were included in PCA: SDEs on soluble sugars and free proline content, antioxidant enzymes activity, photosynthetic pigments, and gas-exchange parameters, including WUE. Four principal components (PCs) accounted for nearly 85% of SDE variability for physiological and biochemical traits (Table 1).

PC 1 with the largest contribution (>30%) was associated mainly with SDE on Chl (*a+b*)/Car, Car, and proline content. PC 2 contributed more than 23% and was associated with SDE on Chl (*a+b*)/Car, sugar content, proline, and GR activity. PC 3 contributed more than 17% to the variability and was associated with SDE on sugar content, Car, and GR activity. PC 4 with the contribution of more than 12% was associated with SDE for pigment content, GR, and SOD activity. Based on PCA results, we identified six traits that determine the variability of adaptive responses to drought in the studied genotypes: Chl (*a+b*)/Car, content of Car, proline, soluble sugars, GR and SOD activity. Positive SDEs for these traits characterize the ability of genotypes to mobilize the physiological and biochemical mechanisms of adaptation to drought.

PCA for SDE on Chl fluorescence parameters: To reduce the number of Chl fluorescence parameters and identify the most variable ones, we applied principal component analysis. PCs were identified that account for a total of 91% of the variability of traits. They include 11 Chl fluorescence parameters: F_m , Φ_{PSII} , ETR, α , ETR_{max} , I_k , ψ_0 , F_v/F_0 , PI_{abs}, RC/ABS, and PI_{tot}, whose positive SDE characterizes a good plant adaptation to stress conditions (Table 2).

Calculation of the comprehensive drought tolerance index *D* and ranking of genotypes: SDE values for biochemical and Chl fluorescence parameters selected by PCA are presented in Tables 3 and 4. Further, based on the selected biochemical traits, we calculated the comprehensive drought tolerance index *D* for each

genotype and ranked the genotypes according to this *D* (Table 5). Higher *D* values are characteristic of more tolerant genotypes. S29, lines S29(YP 2B), and S29(Caez. 2D) with the highest *D* values in the rating were identified as the most tolerant. By the size of SDE on shoot biomass (Fig. 1A), these genotypes were also identified as the most tolerant. They lost no more than 25% of the mass of the main shoot during drought. Line S29(483 2A) which has the lowest *D* index, was determined as the least tolerant both in terms of biochemical parameters and the size of the drought effect on shoot biomass. It lost up to 47% of the shoot biomass in drought. The comprehensive drought tolerance index *D* was positively correlated with the SDE on shoot biomass ($R = 0.67, p < 0.05$). The most significant negative SDE for the Chl (*a+b*)/Car trait also was observed in S29(483 2A) (Table 3).

Similarly, using SDE values for the eleven selected fluorescence parameters, we calculated the comprehensive tolerance index *D* for each genotype and ranked the genotypes according to this *D* (Table 5). Line S29(YP 2B), S29, and line S29(Caez. 2D) showed the highest *D* values, from 0.743 to 0.832, which we defined as drought-tolerant genotypes. Caez. and line S29(483 2A), having the lowest *D* values, from 0.254 to 0.315, were identified as non-drought tolerant genotypes. The index *D* calculated from SDE on Chl fluorescence parameters, was positively correlated with SDE on shoot mass ($R = 0.75, p < 0.01$).

Correlations among SDEs for biochemical and Chl fluorescence parameters: Analysis of the correlations among SDEs for Chl fluorescence and biochemical parameters revealed a total of 18 associations. Fourteen of them were positive and four were negative (Table 6).

Table 1. Principal component analysis of size of drought effect on physiological and biochemical traits. Car – carotenoids; GR, SOD – glutathione reductase and superoxide dismutase activity.

Principle component, PC	Contribution to total variation [%]	Contribution in PC
1	31.3	Chl (<i>a+b</i>)/Car (0.74); Car (-0.59); Proline (0.26)
2	23.7	Chl (<i>a+b</i>)/Car (0.52); Sugars (0.43); GR (-0.31); Proline (-0.25)
3	17.7	Sugars (0.81); GR (0.36); Car (-0.32)
4	12.2	GR (0.71); Car (0.47); SOD (-0.24); Chl (<i>a+b</i>)/Car (0.23)

Table 2. Principal component analysis of size of drought effect on Chl fluorescence parameters. α – the angle of inclination of the light curve characterizing the dependence of fluorescence on light intensity; ETR – rate of electron transfer; ETR_{max} – maximal electron transport rate; F_m – maximal Chl fluorescence; F_v/F_0 – ratio of photochemical to nonphotochemical quantum efficiencies; I_k – the light intensity at which the alpha (α) and ETR lines intersect; PI_{abs} – performance index at absorption basis; PI_{tot} – total performance index; RC/ABS – efficiency indicator, expressed as the concentration of reaction centers in the total pool of chlorophyll; ψ_0 – efficiency with which a trapped excitation can move an electron in the electron transport chain further than Q_A ; Φ_{PSII} – effective quantum yield of PSII photochemistry.

Principle component, PC	Contribution to total variation [%]	Contribution in PC
1	41.6	ETR_{max} (0.38); ETR (0.37); I_k (0.37); Φ_{PSII} (0.30); ψ_0 (0.29); PI _{abs} (0.29); α (-0.28); PI _{tot} (0.24)
2	24.6	ETR_{max} (0.65); α (0.55); I_k (0.40); F_v/F_0 (0.21)
3	17.7	F_m (0.75); ETR_{max} (0.47); I_k (0.27); Φ_{PSII} (0.23); F_v/F_0 (0.22)
4	7.1	PI _{abs} (-0.51); ψ_0 (-0.50); ETR (0.44); Φ_{PSII} (0.36); RC/ABS (0.27); α (0.23)

Table 3. The size of drought effect (SDE) on biochemical indicators used to calculate the *D* index in the genotypes studied. **p*<0.05, ***p*<0.01, ****p*<0.001 – the significance of the difference in means between control and drought. Car – carotenoids; GR, SOD – glutathione reductase and superoxide dismutase activity.

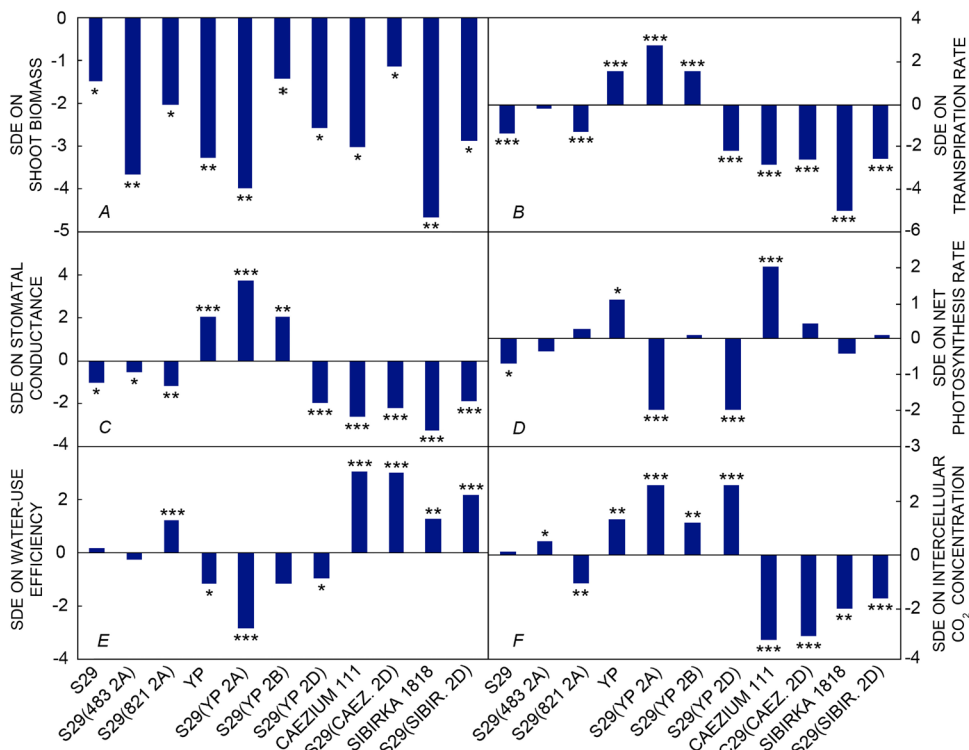
	S29	YP	Caezium 111	Sibirka 1818	S29(YP 2A)	S29(YP 2B)	S29(YP 2D)	S29(Caez. 2D)	S29(483 2D)	S29(483 2A)	S29(821 2A)
Proline	3.2*	-10.9***	8.9**	8.4**	8.2**	9.8***	5.7**	12.6***	1.6	6.1**	15.1***
Soluble sugars	5.8***	-0.9	-4.0***	-7.1***	-5.2***	1.4*	-2.4***	-10.9***	-1.6*	-3.3**	-0.3
GR	-0.2	1.6	1.1	-2.4	0.6	18.9*	-0.6*	3.0*	3.6	-	-1.0
SOD	-1.0	-2.0*	-0.5	2.1*	3.1*	-1.5	-0.6	3.4	5.2**	-	0.8*
Car	0.0	-	9.5**	2.7**	0.0	19.0***	9.5**	-9.5**	9.5**	0.0	0.0
Chl (a+b)/Car	20.0***	-	2.4	6.7**	6.8**	7.6***	4.8*	12.4***	4.6**	-15.0***	7.1***

Table 4. The size of drought effect (SDE) on fluorescent indicators used to calculate the *D* index in the genotypes studied. **p*<0.05, ***p*<0.01, ****p*<0.001 – the significance of the difference in means between control and drought. α – the angle of inclination of the light curve characterizing the dependence of fluorescence on light intensity; ETR – rate of electron transfer; ETR_{max} – maximal electron transport rate; F_m – maximal Chl fluorescence; F_v/F₀ – ratio of photochemical to nonphotochemical quantum efficiencies; I_k – the light intensity at which the alpha (α) and ETR lines intersect; PI_{abs} – performance index at absorption basis; PI_{tot} – total performance index; RC/ABS – efficiency indicator, expressed as the concentration of reaction centers in the total pool of chlorophyll; ψ_0 – efficiency with which a trapped excitation can move an electron in the electron transport chain further than Q_A; Φ_{PSII} – effective photochemical quantum yield of PSII.

	S29	YP	Caezium 111	Sibirka 1818	S29(YP 2A)	S29(YP 2B)	S29(YP 2D)	S29(Caez. 2D)	S29(483 2D)	S29(483 2A)	S29(483 2A)
F _m	0.97***	0.00	0.26	0.15	-0.24	0.25	0.04	0.34*	-0.15	1.00***	1.00***
Φ_{PSII}	0.60**	0.70**	-0.01	0.04	0.10*	0.90***	0.10*	0.70***	0.56**	0.00	0.00
ETR	0.56**	0.75**	0.00	0.04	0.39*	0.88***	0.41*	0.75***	0.53**	0.04	0.04
α	0.71**	0.13	-0.03	-0.10	0.07	-0.35	0.53**	0.23	1.07***	0.17	0.17
ETR _{max}	0.60**	0.34*	0.16	0.11	0.42*	1.48***	0.00	0.57**	0.10	-0.08	-0.08
I _k	0.20	0.31*	0.10	-0.01	0.42*	1.00***	-0.42*	0.33	0.02	-0.20	-0.20
ψ_0	0.35*	-0.17	-0.09	0.61**	0.03	0.59**	-0.12	0.36**	0.04	-0.42*	-0.42*
RC/ABS	0.36*	0.69**	0.20	0.24	0.40*	0.11	0.63**	0.83***	0.54**	0.14	0.14
F _v /F ₀	1.04**	0.70**	-0.26	0.62**	0.55**	0.47*	0.36*	0.55**	1.51***	0.26	0.26
PI _{abs}	0.89***	0.90**	0.07	1.22***	1.14***	0.56*	0.35*	1.13***	0.10	0.10	0.10
PI _{tot}	0.23	0.22	0.24	-0.10	0.25*	0.24*	-0.27*	-0.16	-0.28*	-0.50*	-0.50*

Table 5. Ranking of genotypes by the comprehensive drought tolerance index D calculated from the size of drought effect (SDE) on biochemical traits and Chl fluorescence parameters.

Ranking from SDE on biochemical traits			Ranking from SDE on Chl fluorescence parameters		
Genotype	Complex index of tolerance D	Ranking	Genotype	Complex index of tolerance D	Ranking
S29(YP 2B)	0.745	1	S29(YP 2B)	0.832	1
S29	0.632	2	S29	0.782	2
S29(Caez. 2D)	0.625	3	S29(Caez. 2D)	0.743	3
S29(821 2A)	0.599	4	YP	0.685	4
S29(YP 2A)	0.528	5	S29(Sib. 2D)	0.603	5
S29(Sib. 2D)	0.501	6	S29(821 2A)	0.522	6
Sibirka 1818	0.485	7	Sibirka 1818	0.472	7
Caezium 111	0.451	8	S29(YP 2A)	0.435	8
S29(YP 2D)	0.390	9	S29(YP 2D)	0.418	9
YP	0.302	10	S29(483 2A)	0.315	10
S29(483 2A)	0.220	11	Caezium 111	0.254	11

Fig. 1. The size of the drought effect (SDE) on shoot biomass (A), transpiration rate (B), stomatal conductance (C), photosynthesis rate (D), water-use efficiency (E), and intercellular CO₂ concentration (F) in the studied wheat genotypes. * $p<0.05$, ** $p<0.01$, *** $p<0.001$ – the significance of the difference in means between control and drought.

Expected positive correlations were found between SDE on Chl ($a+b$)/Car and Φ_{PSII} , q_p and ETR_{max} . SDE on free proline content in leaves did not correlate with the same for Chl fluorescence parameters, in contrast to soluble sugar content, which SDE positively correlated with SDE on F_t , F_m , and $F_{300\text{ }\mu\text{s}}$ after the start of plant illumination. Nine correlations were found between SDE on ascorbate–glutathione cycle enzyme activity and Chl fluorescence parameters. There was a strong positive correlation between SDE on DHAR activity and PI_{tot} , an indicator

of the functional activity of PSII, PSI, and the electron transport chain between them. SDE on I_k correlated with SDE on the three enzymes of the ascorbate–glutathione cycle: DHAR, GR, and APX.

Gas-exchange parameters: Genotypes differed in response of stomatal apparatus to drought. The varieties Caez., Sib., S29, and 2D chromosome-substitution lines responded to drought with a sharp decrease in E and g_s . These parameters, on the contrary, increased in YP and lines

S29(YP 2A), S29(YP 2B) (Fig. 1B,C). Cv. Caez. showed the largest (+2) SDE on P_N which resulted in the highest WUE for this cultivar. Based on the WUE parameter, the tolerant varieties are Caezium 111, Sibirka 1818, and the lines S29(Caez. 2D), S29(Sibir. 2D), and S29(821 2A). Variety S29 and line S29(483 2A) exhibited stable and comparable WUE values. YP and line S29(YP 2A) are non-tolerant to drought according to WUE (Fig. 1E).

Comparison of productivity components for variety S29 and line S29(483 2A) grown under optimum and deficit-water conditions: To compare productivity components, we selected genotypes with similar SDEs on WUE (Fig. 1) but contrasting in drought tolerance indices D ratings. In these ratings, we defined the variety S29 with high D indices (0.632 and 0.782) as a tolerant genotype and the line S29(483 2A) with low D indices (0.220 and 0.315) as a non-tolerant one.

Table 6. *Spearman* correlation coefficients among sizes of drought effect for shoot biomass, biochemical and Chl fluorescence parameters. *, ** and *** – correlations are significant at 5, 1 and 0.1% significance levels. Car – carotenoids; DHAR, GR, APX, SOD – dehydroascorbate reductase, glutathione reductase, ascorbate peroxidase, and superoxide dismutase activity; α – the angle of inclination of the light curve characterizing the dependence of fluorescence on light intensity; ETR – rate of electron transfer; ETR_{max} – maximal electron transport rate; F_t – terminal steady state of Chl a fluorescence; F_m' – maximal Chl fluorescence in leaves adapted to light; F_v/F_m – maximal photochemical efficiency of PS II; F_v/F_0 – ratio of photochemical to nonphotochemical quantum efficiencies; $F_{300\mu s}$ – fluorescence measured 300 μs after the start of illumination; I_k – the light intensity at which the alpha (α) and ETR lines intersect; PI_{tot} – total performance index; q_p – coefficient of photochemical fluorescence quenching; V_1 – relative value of variable fluorescence during phase I (30 ms); Φ_{PSII} – effective quantum yield of PSII photochemistry.

	Shoot biomass	Soluble sugars	DHAR	GR	APX	SOD	Car	Chl ($\alpha+b$)/Car
F_v/F_m	-	-	-	-	-	-	-0.82**	-
F_t	-	0.63*	-	-	-	-	-	-
F_m'	-	0.83**	-	-	-	-	-	-
Φ_{PSII}	0.63*	-	-	0.75*	-	-	-	0.65*
q_p	-	-	-	-	-	-	-	0.70*
ETR	-	-	-	0.72*	-	-	-	-
α	-	-	-0.77**	-	-	-	-	-
ETR_{max}	-	-	-	-	-	-	-	0.87***
I_k	-	-	0.76**	0.67*	0.69*	-	-	-
$F_{300\mu s}$	-	0.62*	-	-	-	-	-	-
V_1	-	-	-0.71*	-	-	0.65*	-	-
F_v/F_0	-	-	-	-	-	-	-0.79**	-
PI_{tot}	-	-	0.88***	-	-	-	-	-

Table 7. Some traits of plants productivity of wheat S29 and line S29 (483 2A) under contrasting watering conditions. Means \pm SD are given, $n = 14$. * $p < 0.05$, ** $p < 0.01$, *** $p < 0.001$ – the significance of the difference in means between S29 and S29(483 2A). SI – sustainability index calculated as: SI [%] = (the value under drought/the value in control) $\times 100$.

Yield components	S29			S29(483 2A)		
	Control	Drought	SI [%]	Control	Drought	SI [%]
Stem length [cm]	98.7 \pm 8.7	100.8 \pm 5.2	102	102.8 \pm 4.2	92.1 \pm 6.0**	89
Spike length [cm]	8.1 \pm 0.5	8.5 \pm 0.7	105	7.9 \pm 0.3*	7.5 \pm 0.5*	95
Grain mass (main ear) [g]	1.1 \pm 0.2	1.1 \pm 0.2	100	0.1 \pm 0.2*	0.9 \pm 0.1***	94
Grain number (secondary ears)	87.4 \pm 17.1	63.4 \pm 8.5	70	71.1 \pm 13.8*	46.6 \pm 18.7*	65
Grain mass (secondary ears) [g]	3.2 \pm 0.7	2.0 \pm 0.4	63	2.6 \pm 0.7	1.3 \pm 0.5**	50
Number of grains per plant	113.0 \pm 20.9	89.6 \pm 11.4	80	97.5 \pm 17.0	73.0 \pm 18.3*	75
Grain mass per plant [g]	4.3 \pm 0.8	3.2 \pm 0.5	74	3.5 \pm 0.9	2.2 \pm 0.5***	63
Mass of 1,000 grains [g]	38.2 \pm 3.3	36.3 \pm 3.2	95	35.6 \pm 3.4	30.9 \pm 3.5**	87

The data in Table 7 show that under conditions of optimum irrigation, line S29(483 2A) differed from variety S29 by reduced productivity indices. The most significant differences were observed under drought conditions. The mass of grain from the main and secondary ears of the line was significantly lower compared to S29. Sustainability indices (SI [%]) for these traits were also lower in line S29(483 2A). The number and mass of grains per whole plant, mass of 1,000 grains, and sustainability indices for these traits were also lower in line S29(483 2A).

Discussion

Our results showed that changes in biochemical indicators of drought tolerance were associated with changes in Chl fluorescence caused by water deficit in soft wheat plants. The positions of the three genotypes with the highest D

index values [S29, S29(YP 2B), and S29(Caez. 2D)] were completely equal, and the positions of line S29(483 2A), which had low D values in two independent rankings, were almost identical. D values correlated positively and significantly with SDE on shoot mass.

Drought-tolerant variety S29 showed an effective adaptation strategy. WUE was maintained at the same level under different water supplies. The Chl a and the Chl $(a+b)/Car$ ratio in this variety increased significantly under drought. F_v/F_0 increased also to 4.06 under drought compared to 2.52 in control. In this case, the electron flow transferred through one reaction center (ET_0/RC) remained almost unchanged due to a significant decrease in energy dissipation. The DI_0/RC index (the total amount of energy dissipated by one RC as heat or fluorescence) decreased from 0.92 in the control to 0.56 under drought. A 12% decrease in minimal Chl fluorescence (F_0) indicated increased efficiency of energy transfer in PSII under drought conditions (Table 1S). This strategy resulted in a significant increase in Φ_{PSII} , ETR, ETR_{max} , as well as performance indices PI_{abs} and PI_{tot} , in S29 under drought conditions.

Another example of a tolerance genotype was line S29(YP 2B), which has the highest D index in two independent ratings and retained 80% of shoot biomass under drought conditions. Under drought, this line increased stomatal conductance and transpiration, thereby increasing intracellular CO_2 concentration and maintaining photosynthesis unchanged, with a slight decrease in WUE. The line was characterized by high productivity (Table 2S, *supplement*). Line S29(YP 2B) was a vivid example of the active mobilization of defense mechanisms during adaptation to drought. It significantly increased the level of enzymatic antioxidant defense and the accumulation of sugars and chlorophylls. At the same time, an increase in the values of Φ_{PSII} , ETR, ETR_{max} , I_k , F_v/F_0 , and performance indices PI_{abs} and PI_{tot} were observed. The third genotype we identified as drought-tolerant by D indices was line S29(Caez. 2D). This line reduced stomatal conductance and transpiration significantly under drought while maintaining the photosynthetic rate unchanged, which resulted in a high WUE. Additionally, the aforementioned biochemical mechanisms were actively involved and Chl fluorescence parameters improved under drought.

Line S29(483 2A) did not differ from S29 in gas-exchange patterns but had the lowest indices in the D ratings (0.220 and 0.315). This line retained slightly more than 50% of the biomass of the main shoot under water deficit. The Chl $(a+b)/Car$ ratio was strongly reduced under drought. This affected the fluorescence parameters, ψ_0 and PI_{tot} decreased statistically significantly. Line S29(483 2A) was identified as non-tolerant, which was confirmed by the data on productivity under greenhouse conditions (Table 7). These data indicate that fluorescent parameters can be a good tool for the identification of the spring wheat genotypes contrasting in physiological drought tolerance.

Correlation analysis revealed a relationship between SDE on Chl fluorescence parameters and biochemical ones such as soluble sugar content, ascorbate–glutathione

cycle enzyme activity, Car content, and Chl $(a+b)/Car$ ratio. A strong positive correlation ($R = 0.88$, $p < 0.001$) was found between SDE on DHAR activity catalyzing Asc recycling, and SDE on PI_{tot} . Efficient regeneration of Asc is probably the main way to maintain its pool in wheat leaves under drought (Bartoli *et al.* 2005). Not only the antioxidant function of Asc is important in maintaining the stability of photosynthetic apparatus under conditions of water deficiency but also the ability to transfer an electron directly to the photosynthetic electron transport chain (Ivanov *et al.* 2014). Panda *et al.* (2021) described the relationship between the stability of photochemical activity and improved redox regulation of Asc in rice genotypes under conditions of water deficiency. Note also the positive correlations between changes in the activity of three antioxidant enzymes (DHAR, GR, and APX) and changes in the I_k index, which characterizes the rapid light curve. These data support the idea that the ascorbate–glutathione cycle is a powerful defense mechanism of the photosynthetic apparatus against oxidative stress (Ivanov *et al.* 2014). In general, our data are in good agreement with the findings of a meta-analysis of published data that plant drought tolerance is closely associated with enhanced regulation of ascorbate-dependent antioxidant activity (Laxa *et al.* 2019).

The positions of genotypes YP, Caez., lines S29(YP 2A), and S29(821 2A) with average values of the D index in two different ratings of drought tolerance were different. To rank such genotypes, it is not enough to be limited to Chl fluorescence parameters.

Conclusion: Chl fluorescence methods make it possible to identify spring wheat genotypes that activate cellular defense mechanisms. An increase in the Chl $(a+b)/Car$ ratio, the accumulation of soluble sugars, and an increase in the enzymes of the ascorbate–glutathione cycle activity had a significant effect on the successful adaptation of wheat to drought. The SDE on ascorbate–glutathione cycle enzyme activity was correlated with SDE on Chl fluorescence parameters. A strong positive correlation was found between SDE on DHAR and PI_{tot} ($R = 0.88$, $p < 0.001$).

Chl fluorescence techniques can facilitate the modulation of plant tolerance through molecular breeding and ultimately minimize yield losses under unfavorable climate conditions. However, to accurately predict the ability of crop plants to tolerate drought, it is necessary to use complex indicators, including additionally gas exchange and productivity.

References

Baier M., Noctor G., Foyer C., Dietz K.-J.: Antisense suppression of 2-cysteine peroxiredoxin in *Arabidopsis* specifically enhances the activities and expression of enzymes associated with ascorbate metabolism but not glutathione metabolism. – *Plant Physiol.* **124**: 823–832, 2000.

Bartoli C.G., Guiamet J.J., Kiddle G. *et al.*: Ascorbate content of wheat leaves is not determined by maximal L-galactono-1,4-lactone dehydrogenase (GalLDH) activity under drought stress. – *Plant Cell Environ.* **28**: 1073–1081, 2005.

Bates L., Waldren R.P., Teare I.D.: Rapid determination of free proline for water-stress studies. – *Plant Soil Environ.* **39**: 205-207, 1973.

Begović L., Galić V., Abićić I. *et al.*: Implication of intra-seasonal climate variation on chlorophyll *a* fluorescence and biomass in winter barley breeding program. – *Photosynthetica* **58**: 995-1008, 2020.

Bolouri-Moghaddam M.R., Le Roy K., Xiang L. *et al.*: Sugar signalling and antioxidant network connections in plant cells. – *FEBS J.* **277**: 2022-2037, 2010.

Botyanszka L., Zivcak M., Chovancek E. *et al.*: Chlorophyll fluorescence kinetics may be useful to identify early drought and irrigation effects on photosynthetic apparatus in field-grown wheat. – *Agronomy* **10**: 1275, 2020.

Bradford M.M.: A rapid and sensitive method for the quantitation of microgram quantities of protein utilizing the principle of protein-dye binding. – *Anal. Biochem.* **72**: 248-254, 1976.

Chen K., Chen L., Fan J.B., Fu J.M.: Alleviation of heat damage to photosystem II by nitric oxide in tall fescue. – *Photosynth. Res.* **116**: 21-31, 2013.

Dąbrowski P., Keutgen A.J., Keutgen N. *et al.*: Photosynthetic efficiency of perennial ryegrass (*Lolium perenne* L.) seedlings in response to Ni and Cd stress. – *Sci. Rep.-UK* **13**: 5357, 2023.

de Lamotte F., Vianey-Liaud N., Duviau M.-P., Kobrehel K.: Glutathione reductase in wheat grain. 1. Isolation and characterization. – *J. Agr. Food Chem.* **48**: 4978-4983, 2000.

Deng Q., Dou Z., Chen J. *et al.*: Drought tolerance evaluation of intergeneric hybrids of BC₃F₁ lines of *Saccharum officinarum* × *Erianthus arundinaceus*. – *Euphytica* **215**: 207, 2019.

Dische Z.: Color reactions of carbohydrates. – In: Whistler R.L., Wolfrom M.L. (ed.): *Methods in Carbohydrate Chemistry*. Pp. 477-512. Academic Press, New York 1962.

Giannopolitis C.N., Ries S.K.: Superoxide dismutases: 1. Occurrence in higher plants. – *Plant Physiol.* **59**: 309-314, 1977.

Goltsev V.N., Kalaji H.M., Paunov M. *et al.*: Variable chlorophyll fluorescence and its use for assessing physiological condition of plant photosynthetic apparatus. – *Russ. J. Plant Physiol.* **63**: 869-893, 2016.

Hammer Ø., Harper D.A.T., Ryan P.D.: PAST: Paleontological statistics software package for education and data analysis. – *Palaeontol. Electron.* **4**: 4, 2001.

Hedges L.V., Olkin I.: Estimation of a single effect size: parametric and nonparametric methods. – In: Hedges L.V., Olkin I. (ed.): *Statistical Methods for Meta-Analysis*. Pp. 75-106. Academic Press, Amsterdam 1985.

Ivanov B.N., Khorobrykh S.A., Kozuleva M.A. *et al.*: [The role of oxygen and its reactive forms in photosynthesis.] – In: Allahverdiev S.I., Rubin A.B., Shuvalov V.A. (ed.): [Modern Problems of Photosynthesis.] Pp. 407-460. Izhevsk, Moscow 2014. [In Russian]

Kalaji H.M., Schansker G., Brestic M. *et al.*: Frequently asked question about chlorophyll fluorescence, the sequel. – *Photosynth. Res.* **132**: 13-66, 2017.

Laxa M., Liebthal M., Telman W. *et al.*: The role of the plant antioxidant system in drought tolerance. – *Antioxidants* **8**: 94, 2019.

Mwadzingeni L., Shimelis H., Tesfay S., Tsilo T.J.: Screening of bread wheat genotypes for drought tolerance using phenotypic and proline analyses. – *Front. Plant Sci.* **7**: 1276, 2016.

Nakano Y., Asada K.: Hydrogen peroxide is scavenged by ascorbate-specific peroxidase in spinach chloroplasts. – *Plant Cell Physiol.* **22**: 867-880, 1981.

Nezhadahmadi A., Prodhan Z.H., Faruq G.: Drought tolerance in wheat. – *Sci. World J.* **2013**: 610721, 2013.

Oguz M.C., Aycan M., Oguz E. *et al.*: Drought stress tolerance in plants: interplay of molecular, biochemical and physiological responses in important development stages. – *Physiologia* **2**: 180-197, 2022.

Osipova S., Permyakov A., Permyakova M.: Drought tolerance evaluation of bread wheat (*Triticum aestivum* L.) lines with the substitution of the second homoelogous group chromosomes. – *Cereal Res. Commun.* **48**: 267-273, 2020.

Osipova S.V., Permyakov A.V., Permyakova M.D., Rudikovskaya E.G.: Tolerance of the photosynthetic apparatus in recombinant lines of wheat, adapting to water stress of varying intensity. – *Photosynthetica* **57**: 160-169, 2019.

Panda D., Mishra S.S., Behera P.K.: Drought tolerance in rice: focus on recent mechanisms and approaches. – *Rice Sci.* **28**: 119-132, 2021.

Pandey A.K., Jiang L., Moshelion M. *et al.*: Functional physiological phenotyping with functional mapping: A general framework to bridge the phenotype-genotype gap in plant physiology. – *iScience* **24**: 102846, 2021.

Peršić V., Ament A., Antunović Dunić J. *et al.*: PEG-induced physiological drought for screening winter wheat genotypes sensitivity – integrated biochemical and chlorophyll *a* fluorescence analysis. – *Front. Plant Sci.* **13**: 987702, 2022.

Pleban J.R., Guadagno C.R., Mackay D.S. *et al.*: Rapid chlorophyll *a* fluorescence light response curves mechanistically inform photosynthesis modeling. – *Plant Physiol.* **183**: 602-619, 2020.

Pshenichnikova T.A., Osipova S.V., Smirnova O.G. *et al.*: Regions of chromosome 2A of bread wheat (*Triticum aestivum* L.) associated with variation in physiological and agronomical traits under contrasting water regimes. – *Plants-Basel* **10**: 1023, 2021.

Rane J., Singh A.K., Tiwari M. *et al.*: Effective use of water in crop plants in dryland agriculture: implications of reactive oxygen species and antioxidative system. – *Front. Plant Sci.* **12**: 778270, 2022.

Rapacz M., Wójcik-Jagla M., Fiust A. *et al.*: Genome-wide associations of chlorophyll fluorescence OJIP transient parameters connected with soil drought response in barley. – *Front. Plant Sci.* **10**: 78, 2019.

Sami F., Yusuf M., Faizan M. *et al.*: Role of sugars under abiotic stress. – *Plant Physiol. Biochem.* **109**: 54-61, 2016.

Sehgal D., Mondal S., Crespo-Herrera L. *et al.*: Haplotype-based, genome-wide association study reveals stable genomic regions for grain yield in CIMMYT spring bread wheat. – *Front. Genet.* **11**: 589490, 2020.

Sieczko L., Dąbrowski P., Kowalczyk K. *et al.*: Early detection of phosphorus deficiency stress in cucumber at the cellular level using chlorophyll fluorescence signals. – *J. Water Land Dev.* **SI**: 176-186, 2022.

Srivastava A., Biswas S., Yadav S. *et al.*: Physiological and thylakoid proteome analyses of *Anabaena* sp. PCC 7120 for monitoring the photosynthetic responses under cadmium stress. – *Algal Res.* **54**: 102225, 2021.

Strasser R.J., Tsimilli-Michael M., Srivastava A.: Analysis of the chlorophyll *a* fluorescence transient. – In: Papageorgiou G.C., Govindjee (ed.): *Chlorophyll *a* Fluorescence: A Signature of Photosynthesis. Advances in Photosynthesis and Respiration*. Pp. 321-362. Springer, Dordrecht 2004.

Szabados L., Savouré A.: Proline: a multifunctional amino acid. – *Trends Plant Sci.* **15**: 89-97, 2010.

Varshney R.K., Tuberrosa R., Tardieu F.: Progress in understanding drought tolerance: from alleles to cropping systems. – *J. Exp. Bot.* **69**: 3175-3179, 2018.

von Wettstein D.: Chlorophyll-letal und der submikroskopische Formwechsel der Plastiden. – *Exp. Cell Res.* **12**: 427-506,

1957. [In German]
 Wang J., Zhang X., Han Z. *et al.*: Analysis of physiological indicators associated with drought tolerance in wheat under drought and re-watering conditions. – *Antioxidants* **11**: 2266, 2022.
 Zhang X., Wang Z., Li Y. *et al.*: Wheat genotypes with higher yield sensitivity to drought overproduced proline and lost minor biomass under severer water stress. – *Front Plant Sci.*

13: 1035038, 2022.
 Živcák M., Brestic M., Balatova Z. *et al.*: Photosynthetic electron transport and specific photoprotective responses in wheat leaves under drought stress. – *Photosynth. Res.* **117**: 529-546, 2013.
 Živcák M., Brestic M., Olšovská K., Slamka P.: Performance index as a sensitive indicator of water stress in *Triticum aestivum* L. – *Plant Soil Environ.* **54**: 133-139, 2008.

Appendix 1. Some parameters used in studying Chl fluorescence. For review see Strasser *et al.* (2004).

Fluorescence parameter	Description
Extracted fluorescence parameters	
F_t	Terminal steady state of Chl <i>a</i> fluorescence
F_m	Maximal fluorescence
F_m'	Maximal Chl fluorescence in leaves adapted to light
$F_{300\mu s}$	Fluorescence measured 300 μ s after the start of illumination
Calculated parameters	
$ETR = \Phi_{PSII} \times 0.84 \times 0.50 \times PPFD$	Rate of electron transfer
$V_1 = (F_t - F_0)/(F_m - F_0)$	Relative value of variable fluorescence during phase I (30 ms)
F_v/F_0	Ratio of photochemical to nonphotochemical quantum efficiencies
$F_v/F_m (\varphi_{po}) = [1 - (F_0/F_m)]$	Maximal photochemical efficiency of PSII
$\Phi_{PSII} = (F_m' - F_t)/F_m'$	Effective photochemical quantum yield of PSII
$q_p = (F_m' - F)/(F_m' - F_0')$	Coefficient of photochemical fluorescence quenching
$\psi_0 = ET_0/TR_0 = 1 - V_1$	The efficiency with which an exciton captured by a reaction center (RC) moves an electron along the chain after Q_A
$M_0 = [4 \times (F_{300\mu s} - F_0)/(F_m - F_0)]$	Initial slope (first 0.3 ms) of the O-J fluorescence rise
$RC/ABS = \varphi_{po} (V_1/M_0)$	The ratio of the total number of active PSII RCs per absorption flux (ABS)
$\delta_{Ro} = (F_m - F_{2\mu s})/(F_m - F_0)$	Probability that an electron from the intersystem electron carriers is transferred to reduce end electron acceptors at the PSI acceptor side
$PI_{abs} = [RC/ABS \times \varphi_{po}/(1 - \varphi_{po}) \times \psi_0/(1 - \psi_0)]$	Performance index (potential) for energy conservation from exciton to the reduction of intersystem electron acceptors
$PI_{tot} = [PI_{abs} \times \delta_{Ro}/(1 - \delta_{Ro})]$	Performance index (potential) for energy conservation from exciton to the reduction of PSI end acceptors

© The authors. This is an open access article distributed under the terms of the Creative Commons BY-NC-ND Licence.